TISSUE ENGINEERING: Part A
Volume 17, Numbers 9 and 10, 2011

DOI: 10.1089/ten.tea.2009.0693

Osteochondral Tissue Formation Through Adipose-Derived Stromal Cell Differentiation on Biomimetic Polycaprolactone Nanofibrous Scaffolds with Graded Insulin and Beta-Glycerophosphate Concentrations

Cevat Erisken, Ph.D.,[1,*] Dilhan M. Kalyon, Ph.D.,[1,2] Hongjun Wang, Ph.D.,[2]
Ceren Örnek-Ballanco, Ph.D.,[2] and Jiahua Xu, Ph.D.[2]

The ability to fabricate tissue engineering scaffolds containing systematic gradients in the distributions of stimulators provides additional means for the mimicking of the important gradients observed in native tissues. Here the concentration distributions of two bioactive agents were varied concomitantly for the first time (one increasing, whereas the other decreasing monotonically) in between the two sides of a nanofibrous scaffold. This was achieved via the application of a new processing method, that is, the twin-screw extrusion and electrospinning method, to generate gradients of insulin, a stimulator of chondrogenic differentiation, and β-glycerophosphate (β-GP), for mineralization. The graded poly(ε-caprolactone) mesh was seeded with human adipose-derived stromal cells and cultured over 8 weeks. The resulting tissue constructs were analyzed for and revealed indications of selective differentiation of human adipose-derived stromal cells toward chondrogenic lineage and mineralization as functions of position as a result of the corresponding concentrations of insulin and β-GP. Chondrogenic differentiation of the stem cells increased at insulin-rich locations and mineralization increased at β-GP-rich locations.

Introduction

Native tissues are heterogeneous in structure and function that allow them to perform their physiological requirements.[1] Transitional interfaces between tissues play especially crucial roles. For example, at the cartilage-to-bone (osteochondral) interface, the extracellular matrix (ECM) components, including cell types,[2] as well as the concentration of mineral particles[3,4] vary as a function of distance to meet the requirements of the complex hierarchical structure of native tissue. Various degenerative diseases, for example, osteoarthritis, deteriorate this structure, and the existing cartilage grafting methods have, so far, not been able to achieve stable integration with the cartilage or subchondral bone,[5] leaving the regeneration of the native osteochondral interface as a significant clinical challenge. This clinical challenge can be addressed using tissue engineering methods provided that the tissue engineering scaffolds can be tailored to promote the mimicking of the gradients found at interfaces, including cellularity and mineral content. One way of creating such gradients involves the use of functionally graded scaffolds that are incorporated with bioactive agents to modulate cell behavior selectively toward desired paths. However, the embedment of bioactive agents into tissue engineering scaffolds in a controlled manner is a challenge requiring specialized tools and processing techniques.[6,7]

Upon the recognition of the benefits of the utilization of signaling molecules in tissue engineering, various types of growth factors have been exogenously added into cell growth media to direct cell behavior. For example, Luo *et al.*[8] supplemented cell culture media with transforming growth factor-beta 1, basic fibroblast growth factor, or hepatocyte growth factor to examine their effects on the proliferation and ECM synthesis behavior of human vocal fold fibroblasts as well as on matrix contraction. In addition, the use of stem cells, which could be differentiated using appropriate mediators, has opened up new avenues in tissue engineering applications.[9–12] Growth factors, including recombinant human insulin-like growth factor 1 and bone morphogenetic protein 2, have been incorporated into scaffolds to induce stem cell differentiation into osteogenic and chondrogenic phenotypes through controlled release.[10,11] Differentiation of

Departments of [1]Chemical Engineering and Material Science and [2]Chemistry, Chemical Biology and Biomedical Engineering, Stevens Institute of Technology, Hoboken, New Jersey.
*Current affiliation: Department of Biomedical Engineering, Columbia University, New York, New York.

human mesenchymal stem cells into osteogenic and chondrogenic lineages using microencapsulated recombinant human bone morphogenetic protein 2 and recombinant human insulin-like growth factor 1 with controlled doses along the length of the scaffold has also been demonstrated.[13] A recent study of Benoit *et al*.[14] has indicated that small-molecule functional groups attached to three-dimensional (3D) substrates can induce selective differentiation of mesenchymal stem cells, suggesting that tissue engineering scaffolds have the potential to induce location-dependent changes in differentiation of stem cells, provided that scaffolds graded with the requisite chemical composition, pore size, and porosity distributions are available. Overall, these challenges are compounded by the urgent need for the translation of laboratory-based and generally labor-intensive, multi-step scaffold preparation techniques into "clinically appropriate larger scale production techniques" that are "reproducible, safe, clinically effective, and economically acceptable."[15]

In this study, nanoparticles of insulin and β-glycerophosphate (β-GP) were incorporated into a nonwoven mat of poly(ε-caprolactone) (PCL) nanofibers in a graded manner, that is, controlled concentration distributions as a function of scaffold thickness. Human adipose-derived stromal cells (h-ADSCs) were cultured on these nonwoven graded mats for probing their effects on the development of cellularity and mineralization. It is hypothesized that the encapsulation of stimulators into biodegradable nanofibers in a spatially controlled manner would guide the selective differentiation of stem cells into chondrocytes and relevant ECM deposition. More specifically, gradients in insulin concentration along the thickness of the scaffolds would induce gradients of number of chondrocytes as well as chondrogenic matrix deposition, the gradients being in line with insulin concentration.

Similarly, the gradients in concentration of β-GP would lead to incremental mineralization in the tissue constructs. The structure generated in tissue constructs could then allow for better mimicking of the biological and physical properties of native osteochondral ECM. The aim of this study are threefold: (i) to create concentration gradients of multiple ingredients, that is, insulin and β-GP, in nanofibrous scaffolds, (ii) to show the functionality of the scaffolds to selectively differentiate the h-ADSCs into chondrocytes in a graded manner as affected by insulin concentration gradient, and (iii) to generate physical mineralization gradients as affected by β-GP. For the fabrication of the graded scaffolds, a recently developed hybrid twin-screw extrusion and electrospinning technology was utilized.[16] This method enables the fabrication of tissue engineering scaffolds with gradients in composition, porosity, wettability, and mechanical properties.[17] This technology is also suitable to translate the laboratory-based and generally labor-intensive, multi-step scaffold preparation techniques into clinically appropriate and economically feasible production scales.

The critical attributes of the materials of the study included the biocompatibility, ease of processability, and release capability of PCL, as well as the abundant availability (from lipoaspirate) and the demonstrated multi-lineage potential (including chondrocytic and osteoblastic lineages[18]) of the h-ADSCs. The use of insulin relied on its demonstrated ability for chondrogenic differentiation of mesenchymal cells.[19,20] Insulin has also been widely used as a supplement to stimulate the differentiation of adipose-derived stem cells,[18] human bone marrow cells,[21] and cartilage progenitor cells[22] into chondrogenic phenotypes. The scaffolds were also incorporated with β-glycerophosphate (β-GP) to promote mineralization,[23] on the basis of elevated local phosphate ion concentrations induced by alkaline phosphatase or modulation of osteoblast function by phosphate ions through increased bone remodeling or collagen synthesis.[24,25]

Materials and Methods

Scaffold fabrication

Continuously graded insulin/PCL/β-GP scaffolds were fabricated using the recently developed hybrid twin-screw extrusion/electrospinning technology.[16] The process consists of a twin-screw extruder with fully intermeshing and corotating screws (Material Processing & Research, Inc.) integrated with a spinneret die with multichannels for flow and shaping, and connected to a high-voltage supply for electrospinning. The tight clearances between screws and the barrel, and between the screws themselves enabled the break-up of agglomerates while keeping additives distributed homogeneously in the suspension. Operation of twin-screw extruder was controlled by the aid of a computerized field-point based data acquisition/process control system. Electrospinning of nanofibers occurred at a potential of 5 kV with a distance of separation of 7.5 cm between the collecting plate and spinneret die, using a spinneret with a die diameter of 0.6 mm. The ability to tightly control the feed rates and operating conditions provides the wherewithal necessary to fabricate tissue engineering scaffolds continuously and reproducibly (versus batch type cyclic processes).

The PCL (Sigma-Aldrich; Catalog# 440744) was dissolved in dichloromethane (DCM) at a ratio of 12:100 (g/mL), and insulin (Sigma-Aldrich; Catalog# I1882) and β-GP disodium salt hydrate (β-GP; Sigma-Aldrich; Catalog# G9891) were added to PCL/DCM solution to obtain ultimate insulin/PCL and β-GP/PCL concentration ratios of 25:75 and 50:50 by weight, respectively. The β-GP was pulverized before use to have a final particle diameter in the range between 100 and 900 nm. Insulin was received in the form of a nanosized powder and was used as procured (Fig. 1c). The insulin/PCL/DCM suspension was fed into the first mixing zone of the extruder into which β-GP/PCL/DCM was also introduced in a time-dependent, that is, continuously increasing, manner, whereas the feed rate of insulin/PCL/DCM was concomitantly decreased. The nonwoven meshes (thickness of $\sim$500 μm) with gradients of concentrations of insulin and β-GP were, then, punched into discs of 8 mm in diameter to be used as scaffolds for culturing of h-ADSCs or for mechanical characterization.

Tissue formation

Discs were first sterilized in 70% ethanol and then washed by immersing in a phosphate-buffered saline (PBS). The h-ADSCs were obtained as part of a series of adipose stromal cells isolated from 13 patients, which were separately tested by Coriell Institute for Medical Research, for their osteogenic, chondrogenic, and adipogenic differentiation. It was determined that 12 of 13 isolations showed similar capacity for osteogenic, chondrogenic, and adipogenic differentiation upon culture in the corresponding differentiation media (private communication). One out of these 12 isolations

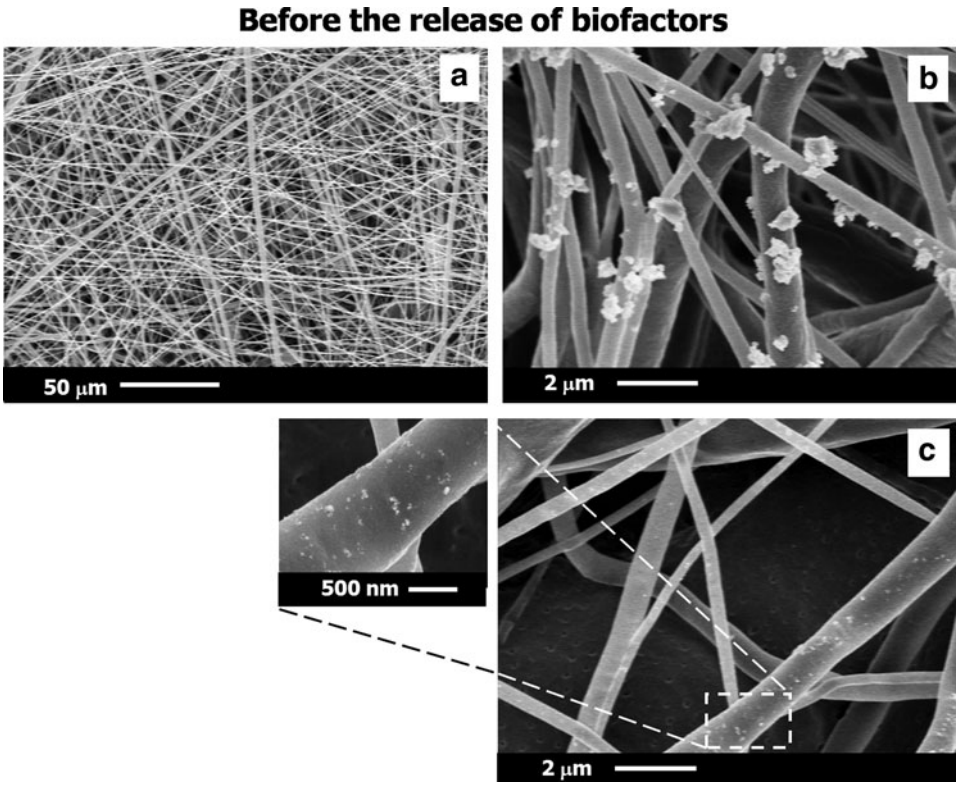

FIG. 1. Scanning electron microscopy micrographs of general surface structure of functionally graded scaffolds (**a**), with higher magnifications of β-GP-rich (**b**), and insulin-rich (**c**) sides. β-GP, β-glycerophosphate.

(obtained from the neck and arms of a 56-year-old woman upon tumescent liposuction from subcutaneous adipose tissue) was used in our study. Cells were proliferated in a low serum (0.5% fetal bovine serum) medium supplemented with epidermal growth factor, platelet-derived growth factor BB, insulin, and transferrin. Before seeding, cells (at passage 5) were detached with 0.25% trypsin–EDTA (Invitrogen; Catalog# R-001-100), centrifuged, and resuspended in combined medium (described below) for homogeneity.

A total of 34,000 cells[17] were seeded onto each side of the scaffolds placed in a 24-well plate. Then, 1 mL of combined medium was added to immerse the scaffolds completely, followed by their culturing in an incubator at 37°C and 5% CO_2. The combined medium was prepared by mixing Minimum Essential Medium (MEM) Alpha Medium (Invitrogen; Catalog# 11900-073), which was supplemented with fetal bovine serum (Invitrogen; Catalog# 16000-036), penicillin/streptomycin (1/0.045/0.01 volume ratio, respectively), and $NaHCO_3$ (2.2 g/L) with Dulbecco's modified Eagle's medium high glucose (Invitrogen; Catalog# 11960-051) supplemented with fetal bovine serum and penicillin/streptomycin (1/0.1/0.01 volume ratio, respectively) by a ratio of 50:50 by volume. MEM Alpha and Dulbecco's modified Eagle's medium high glucose were successfully used earlier for osteoblastic[26] and chondrogenic[27] differentiation, respectively, in conjunction with various types of stem cells, including human adipose-derived stem cells. The medium was replaced every other day, and cell–scaffold constructs were flipped upon every change of the medium. Such flipping of scaffolds was carried out to reduce the sedimentation of the cells. Resulting tissue constructs were harvested after 1, 4, and 8 weeks and were kept in 4% buffered formaldehyde solution until characterization.

Scaffold characterization

A LEO Gemini 982 scanning electron microscope was used for the characterization of the nanofiber diameters, pore size, and the surface attributes of electrospun meshes. The presence of β-GP was assessed via Na and P scans at 10 kV. The spatial distributions of the concentrations of insulin and β-GP in the scaffolds were measured by using a thermo gravimetric analysis, TGA, apparatus (TGA-Q50, TA Instruments). The TGA experiments were carried out by heating of the specimens collected from different locations in the scaffolds from 25°C to 590°C at a constant rate of 15°C/min under N_2 atmosphere.

Tissue processing and characterization

Fixed tissue constructs were dehydrated using a series of increased concentrations of ethanol and kept overnight under vacuum. For scanning electron microscopy (SEM) characterization, the specimens were mounted on Al stubs, coated with Au, and analyzed using a LEO Gemini 982 scanning electron microscope. For histological analyses, the harvested tissue constructs were embedded in a glycol methacrylate-based embedding material, that is, Immuno-Bed (Polyscience, Inc.). Thin sections (5 μm) were obtained from tissue constructs embedded in plastic and stained with hematoxylin and eosin (H&E) to examine the cell distribution and chondrocyte-specific cell morphology. Glycosaminoglycan (GAG) and collagen depositions by chondrocytes were evaluated after 4 weeks using Alcian Blue (AB) and picrosirius red stains, respectively. The intensity of the stain over the entire tissue constructs was quantified using ImageJ software. To further probe the differentiation of h-ADSCs into chondrogenic phenotype, tissue constructs after 1 and 8 weeks of cell culture

were permeabilized and incubated with a goat polyclonal anti-melanoma-inhibiting activity (MIA), a rabbit polyclonal anti-activin receptor-like kinase (ALK)-1, and anti-fibroblasts growth factor receptor 3 (FGFR3), and subsequently FITC-conjugated secondary antibodies. Samples were imaged using a Zeiss LSM510 confocal microscope. Z-stack feature was used to detect the spatial distribution of the chondrocytic differentiation within the tissue constructs. Sections were also treated with $AgNO_3$ solution and subjected to strong light (i.e., von Kossa stain) to evaluate the presence of Ca. The stained sections were analyzed using a Nikon Polarizing Microscope (Micron Optics). The distribution of mineral deposition over the entire scaffolds and time were evaluated by quantifying the stain intensity using ImageJ software.

Native cartilage-bone specimen preparation

Fresh bovine knee joints (6 months old) were obtained from a local abattoir and stored at −80°C. The joints were thawed at room temperature for ~12 h and femoral condyles were drilled to a depth of ~3 mm to remove the native osteochondral tissue. The specimens were equilibrated in PBS solution at 4°C. Thicknesses were measured at four different locations and samples with 100 μm or more variations were discarded.

Biomechanical characterization

Unconfined uniaxial compression testing of engineered tissue constructs and the native osteochondral tissue were performed using a Rheometric Scientific ARES Rheometer (currently TA Instruments) in the strain amplitude range of 0% to 10%. The specimens while in their fresh state were first equilibrated under a tare load and then compressed at a constant rate of 0.05 mm/s. The modulus and toughness values were determined from the slope of stress versus strain behavior and the area under the stress versus strain curve, respectively. To prevent dehydration during tests, specimens were deformed within a custom-designed environmental chamber[28] filled with PBS and kept at 37°C.

Statistical analysis

All statistical analyses were performed using SPSS 13.0 statistical software. Assumptions of normality and homogeneity of variance were verified by using Shapiro-Wilks's test and Levene's test, respectively, and homogeneity of group covariance matrices was verified by using Box's M test. Statistical significance for the change of insulin and β-GP concentrations as well as mineral distributions along the thickness of scaffolds was investigated using one-way multivariate analysis of variance (ANOVA). Significant multivariate omnibus test statistics were followed by univariate analyses. Type I error was controlled by employing the Bonferroni correction and testing each ANOVA at a significance (alpha) level of 0.025 (i.e., $p = 0.05/2$). The Bonferroni *post-hoc* procedure was then used to test for significance in cases of multiple comparisons. The distributions of chondrocytic cell count, GAG, and collagen deposition along the length of tissue constructs were examined through one-way ANOVA, followed by Tukey's *post hoc* comparisons. The mineral deposition over time was evaluated using Student's *t*-test.

Results

Scaffold fabrication and characterization

Scaffolds consisting of highly porous nonwoven meshes with pore sizes ranging between 5 and 50 μm and fiber diameters in the range of 200 to 2000 nm were fabricated and are shown in Figure 1a. Bottom, β-GP-rich, and top, insulin-rich, sides of the typical scaffolds are also shown in Figure 1b and c, respectively. Location-dependent thermo-gravimetric characterization of the scaffold meshes validated that indeed continuous concentration gradients of both insulin and β-GP could be achieved along the thickness of the scaffolds (i.e., along 500 μm). The concentration of insulin increased linearly from 0% to 23.2% ± 2.6% by weight from one side of the scaffold to the other, whereas the β-GP concentration decreased from 48.3% ± 2.8% to 0% by weight along the same direction (Fig. 2a). The concentration (weight fraction) of β-GP at the bottom of the scaffold (48.3% ± 2.8%, $n = 3$) is significantly higher than that of β-GP at 175 μm (14.1% ± 0.7%, $n = 3$; $p = 0.000$), and that of β-GP at 300 μm (1.0% ± 1.0%, $n = 3$; $p = 0.000$). Similarly, the concentration of insulin at the top of the scaffold (23.2% ± 2.6%, $n = 3$) is significantly higher than that of insulin at 300 μm (15.8% ± 3.1%, $n = 3$; $p = 0.002$), and at 175 μm (7.8% ± 0.5%, $n = 3$, $p = 0.000$). Energy dispersive spectra provided collaborative data, that is, decreasing intensities of Na and P peaks, characteristic of β-GP, with increasing distance from the bottom of electrospun mesh, indicative of the decreasing concentration of β-GP (Fig. 2b).

PCL scaffolds containing either only β-GP or only insulin were also fabricated and immersed in cell culture media to evaluate the time-dependent release of β-GP and insulin. The release study was carried out to determine the concentrations of bioactive agents to be incorporated into the PCL scaffolds. The weight loss of the scaffolds containing 23% wt insulin is

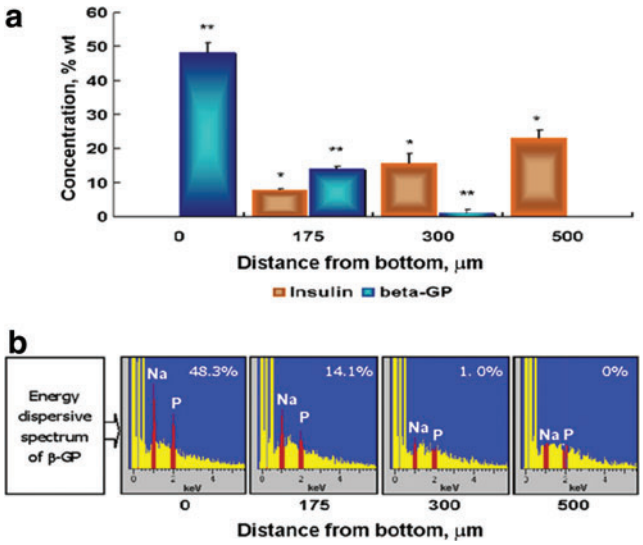

FIG. 2. Thermo gravimetric analysis, TGA (**a**) and energy dispersive spectroscopy, EDS (**b**) characterization for the concentration distribution of bioactive agents. Symbols * and ** indicate significance at $p < 0.025$ for insulin and β-GP, respectively, for $n = 3$. Error bars represent standard error (s.e.m.) at 97.5% confidence level. Color images available online at www.liebertonline.com/tea

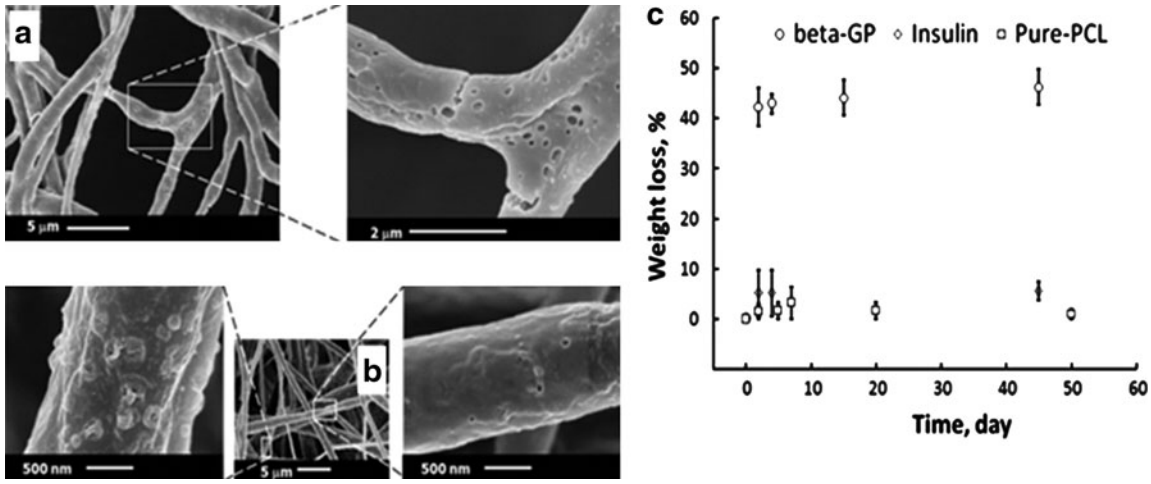

FIG. 3. Scanning electron microscopy micrographs of surface structure of β-GP-rich (**a**), and insulin-rich (**b**) sides after the release of bioactive agents together with weight-based release profile for a duration of 6 weeks (**c**).

5% in two days (Figure 3c), which corresponds to the release of about 22% of the insulin initially loaded, assuming that the PCL is not affected. There is negligible release of the insulin after two days. It was observed that β-GP, which is a hydrophilic Na salt, released at a higher rate in the media due to its greater dissolution rate.[29] After 6 weeks, the surface morphology of scaffolds was observed to change from smooth to irregular and also to exhibit surface voids (Fig. 3). Surface porosity was more prominent on the β-GP-rich side (Fig. 3a), associated with greater dissolution rate (Fig. 3c) of the hydrophilic Na salt, that is, β-GP, in comparison to insulin.

Tissue formation and SEM characterization

Attachment, proliferation, and differentiation behavior of h-ADSCs were investigated during the 8 weeks of culturing. SEM characterization of tissue constructs revealed that cells attached well over the entire length of the scaffold (Fig. 4a, d), and cell proliferation took place with multiple cell layers forming at the sides (Fig. 4b, e) and interior volume, that is, the "core," of the scaffolds (Fig. 4c, f, g). The formation of collagen fibril bundles (inset to Fig. 4c) is apparent in insulin-rich side after 8 weeks of culture.

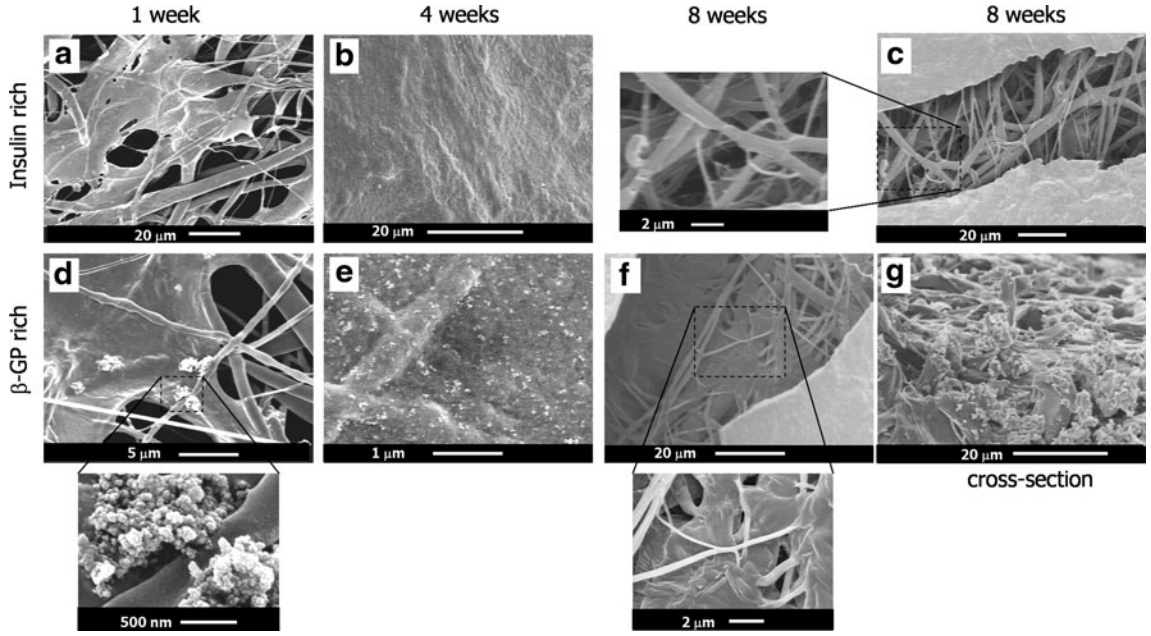

FIG. 4. Extracellular matrix formation and mineralization of tissue constructs. Cells adhered well to both sides of scaffolds after 1 week (**a, d**). Globular particulates (supposedly minerals) are apparent in β-GP-rich side (**d**), whereas no particulates were observed in insulin-rich side (**a**). After 4 weeks, surfaces of scaffolds were covered with layers of cells (**b, e**) with greater particulate deposition in β-GP-rich side (**e**). After 8 weeks, formation of extracellular matrix (**c, f**) and fibrils (inset to **c**) revealed further development of tissue. Cross section of tissue constructs after 8 weeks (**g**) also indicated formation of rich and highly mineralized extracellular matrix in β-GP-rich side.

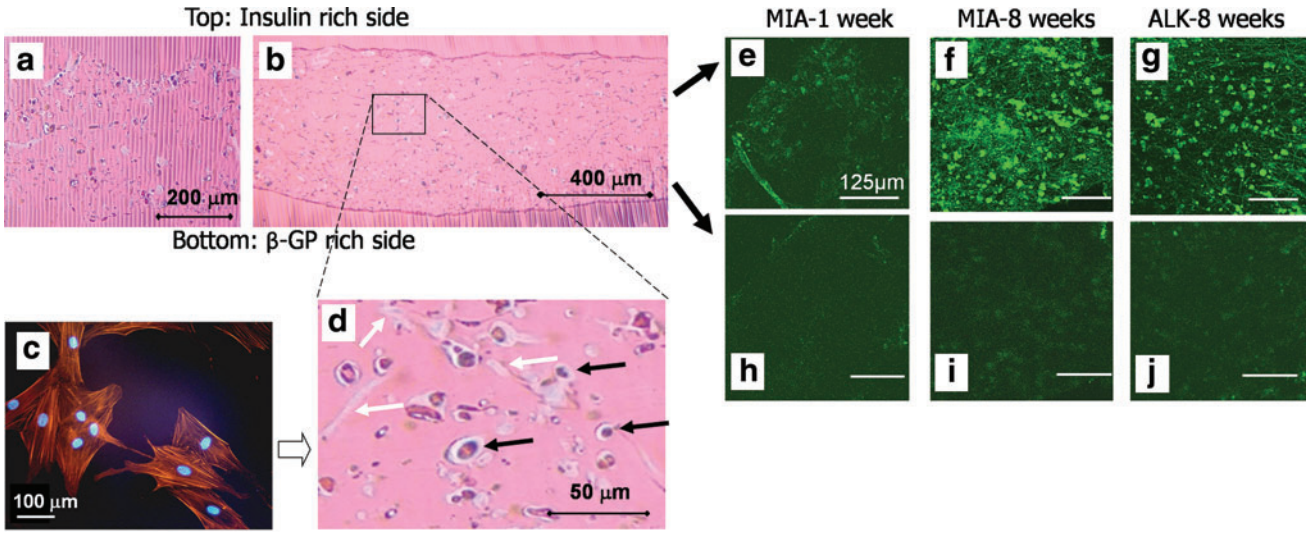

FIG. 5. Hematoxylin and eosin staining showed proliferation and differentiation of h-ADSCs after 1 week (**a**) and 8 weeks (**b**). Differentiation to chondrocyte-specific round morphology (shown with black arrows in **d**) from h-ADSCs (**c**, monolayer, stained with TRITC-conjugated phalloidin for filament-actin [Red/Orange] and DAPI for cell nucleus [blue]) is evident, although some h-ADSCs (white arrow in **d**) remained undifferentiated. Chondrogenic differentiation of h-ADSCs was also demonstrated by immunostaining for melanoma-inhibiting activity (MIA) (top: **e**, **f**; bottom: **h**, **i**). Confocal microscopy analysis showed increasing intensity of MIA immunostaining on the top section of scaffold as a function of time (**e, f**). Two morphologically distinct cell populations, that is, differentiated and dedifferentiated chondrocytes, were immunodetected with ALK-1 (**g, j**). Cells with predominantly round morphology are shown in (**g**). h-ADSC, human adipose-derived stromal cell; ALK, activin receptor-like kinase. Color images available online at www.liebertonline.com/tea

The formation of globular mineral particulates (Fig. 4d, e, g) in β-GP-rich regions suggested that β-GP was indeed effective in promoting the greater extent of mineralization of tissue constructs at locations where it was readily available.

Histology and immunohistochemistry

H&E staining was performed on tissue constructs after 1 and 8 weeks of cell culture and the results are shown in Figure 5a, b, and d. Cells with distinctly different morphologies in-

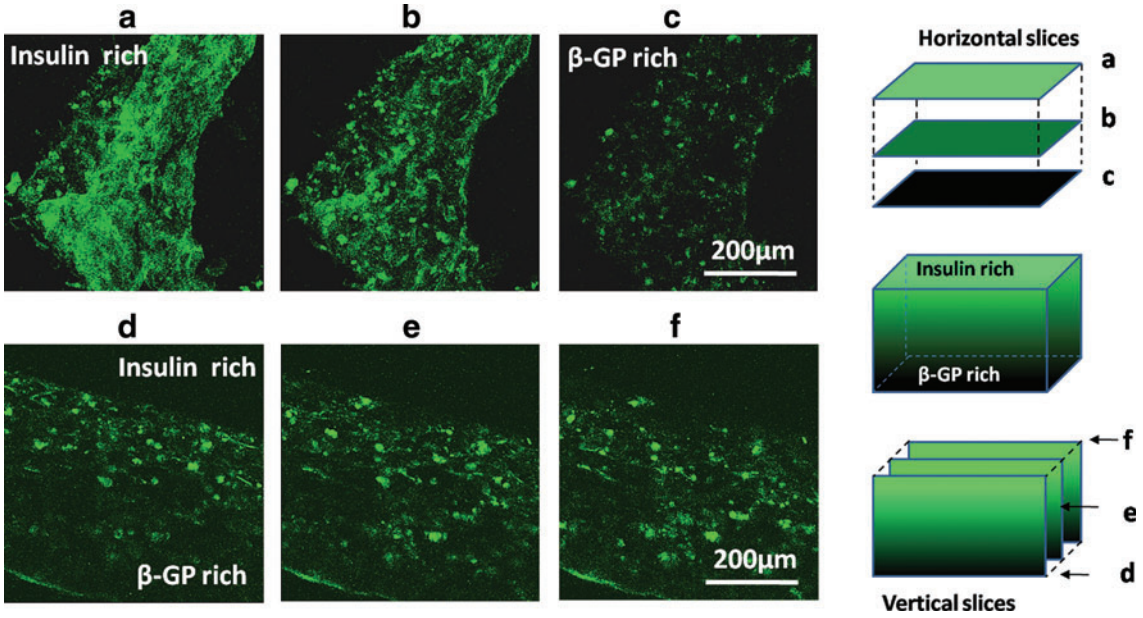

FIG. 6. Immunostaining for FGFR3 after 8 weeks. (**a–c**) Horizontal slices demonstrating depth-dependent change in FGFR3 intensity over the scaffold (insulin rich to β-GP rich from left to right), and (**d–f**) vertical cross sections of the scaffold showing depth-dependent variation in FGFR3 intensity (top: insulin rich, bottom: β-GP rich). FGFR3, fibroblasts growth factor receptor 3. Color images available online at www.liebertonline.com/tea

volving the characteristic round shape of the chondrocytes and the h-ADSCs (Fig. 5c) are observed. The chondrocytic differentiation of h-ADSCs was further confirmed with detection of two type II collagen-coexpressing chondrogenesis markers, MIA[30–33] and FGFR3.[34–38] Confocal microscopy analysis showed the degree of intensity of both markers on the tissue constructs as a function of insulin/β-GP gradient (Figs. 5e, f, 6). Increasing intensity of MIA immunostaining was observed on the top section of scaffold (insulin-rich) in week 8 constructs (Fig. 5e, f). Vertical and horizontal sections of week 8 constructs stained with FGFR3 demonstrated the highest FGFR3 intensity on the insulin-rich sections (Fig. 6a–c), and a clear gradient of FGFR3 intensity proportional with the gradient of insulin concentration (Fig. 6d–f). A 3D construction of the FGFR3 intensity over the entire scaffold is also provided as Supplementary Movie S1 (Supplementary Data are available online at www.liebertonline.com/tea). As differentiated chondrocytes are characteristically unstable by undergoing dedifferentiation and/or re-differentiation,[39–43] phenotypic stability of chondrocytes was also evaluated by immunostaining the tissue constructs (Fig. 5g, j) with ALK-1, a marker of dedifferentiated chondrocytes.[34] ALK-1 was detected in two morphologically distinctive cell populations, that is, differentiated and dedifferentiated chondrocytes, in the 8-week tissue constructs corresponding to the gradient of insulin and β-GP.

The number density of chondrogenic cells (with characteristic round shapes) increased with distance from the bottom surface of tissue constructs, consistent with the monotonic increase of insulin concentration over the same region (Fig. 7a). The number density of these cells correlated positively ($r^2 = 0.95$) with concentration of insulin (Fig. 7b), suggesting that the local availability of insulin was effective in promoting the preferential differentiation of stromal cells. The count of chondrocyte-like cells showed that the number of chondrocytes located at distances in the range of 330 to 500 μm from bottom, that is, $39.64\% \pm 2.54\%$, is significantly greater than those located at distances between 220 and 330 μm from the bottom surface of the scaffold, that is, $24.23\% \pm 0.85\%$ ($n_1 = n_2 = 6$, $\alpha = 0.05$, $p = 0.000$). Similarly, the number of chondrocytes located at distances between 220 and 330 μm from bottom were found to be significantly greater than those located at distances between 110 and 220 μm, that is, $19.46\% \pm 1.73\%$ ($n_1 = n_2 = 6$, $\alpha = 0.05$, $p = 0.006$).

The AB stains performed on tissue constructs after 4 weeks of culturing (Fig. 8a) suggested greater (yet statistically insignificant, $p > 0.05$) staining intensity for sulfated GAG with increasing insulin concentration (Fig. 8b). On the other hand, the picrosirius red stain (Fig. 8c) revealed statistically significant effect of increasing insulin concentration on increasing total collagen deposition (Fig. 8d). The von Kossa stains performed on tissue constructs after 1 week (Fig. 9a) and 8 weeks (Fig. 9b) of culturing showed positive staining for $Ca_3(PO_4)_2$. β-GP incorporated into the nanofibers of our scaffolds generally gave rise to an apparent trend of greater mineral deposition at β-GP-rich locations (Fig. 9c) and over time (Fig. 9d).

Biomechanical characterization

The comparisons of compressive properties of tissue constructs obtained at different culture durations versus those of native bovine osteochondral tissue are shown in Figure 10. Engineered tissue constructs and the native tissue both exhibited linear behavior in 0% to 10% strain amplitude range upon compression at 0.05 mm/s. Compression, at 10% strain, of tissue constructs obtained after 1, 4, and 8 weeks yielded normal stress values of 0.674 ± 0.06, 0.852 ± 0.121, and 1.916 ± 0.100 kPa, respectively. Significantly higher modulus (slope of stress versus strain curve) and toughness (area under stress versus strain curve) values were obtained after 8 weeks of cell culture as compared to those obtained after 1 and 4 weeks, suggesting a considerable degree of tissue formation within 8 weeks (Fig. 10b, c). The modulus values of the native tissue, that is, 20.9 ± 0.15 kPa, were greater than those of engineered tissue constructs at 8 weeks, that is, 0.19 ± 0.01 kPa. Similarly, the modulus values of engineered tissue constructs at 8 weeks were greater than those of engineered tissue constructs at 4 weeks, that is, 0.09 ± 0.01 kPa. As for toughness, the values of native tissue, that is, 1023 ± 33 kPa, were greater than those of engineered tissue constructs at 8 weeks, that is, 9.64 ± 0.70 kPa. Similarly, toughness values of engineered tissue constructs at 8 weeks

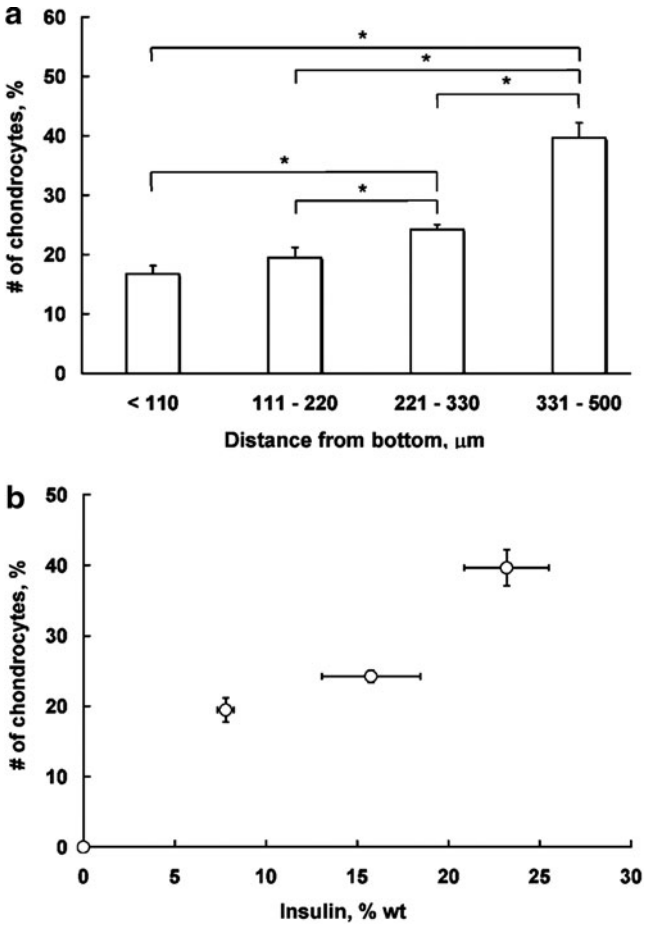

FIG. 7. Count of chondrocyte-like cells (**a**) showed that the number of chondrocytes increased from the bottom of the scaffolds to the top. Symbol * indicates significance at $p < 0.05$ for $n = 6$. Error bars represent s.e.m. at 95% confidence level. There was appreciable correlation ($r^2 = 0.95$) between cell frequency and insulin concentration along the scaffold thickness (**b**).

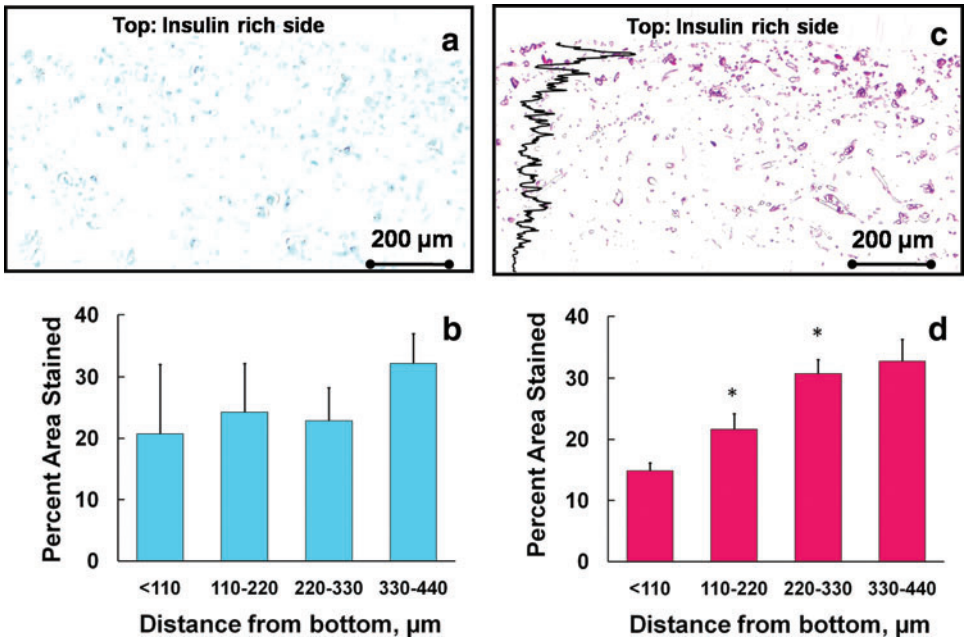

FIG. 8. Alcian Blue stain (**a**) and picrosirius red stain (**c**) after 4 weeks revealed glycosaminoglycan (**b**) and increasing collagen (**d**) deposition as a function of increasing insulin concentration from bottom to top. Symbol * indicates significance between consecutive locations. Error bars represent s.e.m. at 95% confidence level ($n = 3$). Color images available online at www.liebertonline.com/tea

were determined to be greater than those of engineered tissue constructs at 4 weeks, that is, 4.53 ± 0.41 kPa.

Discussion

Aiming at hierarchical structures of interfaces, scaffolds that were spatially organized in the form of distinct multi-layers[5,23,44–48] have been fabricated and culturing of single[44] or multiple[5,46] cell types on these multi-layered scaffolds have been studied. Schaefer *et al.*,[46] for example, prepared two individual sheets consisting of polyglycolic acid on one side and a blend of poly-lactic-co-glycolic acid (PLGA) and polyethylene glycol on the other, and then seeded the two sides with chondrocytes and periosteal cells, respectively. The two constructs were then sutured together after 1 week of culture period to obtain 3D cartilage–bone composites. Later, Sherwood *et al.*[47] designed and manufactured cartilage/bone scaffolds by layering three different materials composed of D,L-PLGA/L-poly(lactic acid) (PLA) for cartilage, L-PLGA/tricalcium phosphate (TCP) for bone, and a blend of these materials for the bone–cartilage transition zone. In another study, Allan *et al.*[23] developed biphasic constructs consisting of cartilaginous tissue anchored to the top surface of a bone substitute with a calcified interface. These constructs were seeded with deep zone chondrocytes from bovine articular cartilage, and cultured in the presence of β-glycerophosphate.

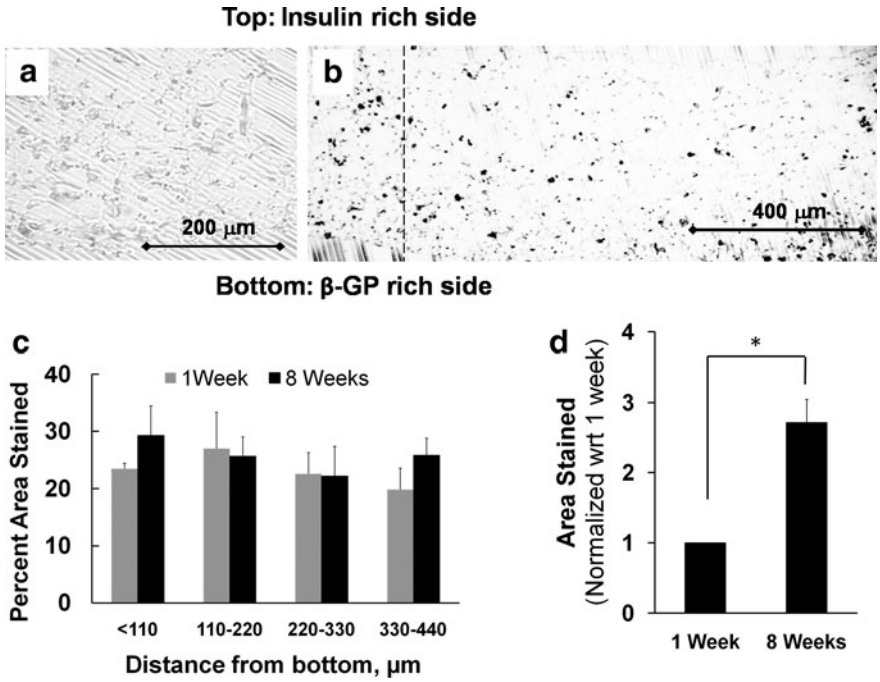

FIG. 9. von Kossa stain after 1 week (**a**) and 8 weeks (**b**) of culture, and mineral deposition as determined by the stained area of sections as a function of scaffold thickness (**c**) and time (**d**). Error bars represent s.e.m. at 97.5% and 95% confidence level for (**c**) and (**d**), respectively, ($n = 3$). Symbol * indicates significance at $p < 0.05$.

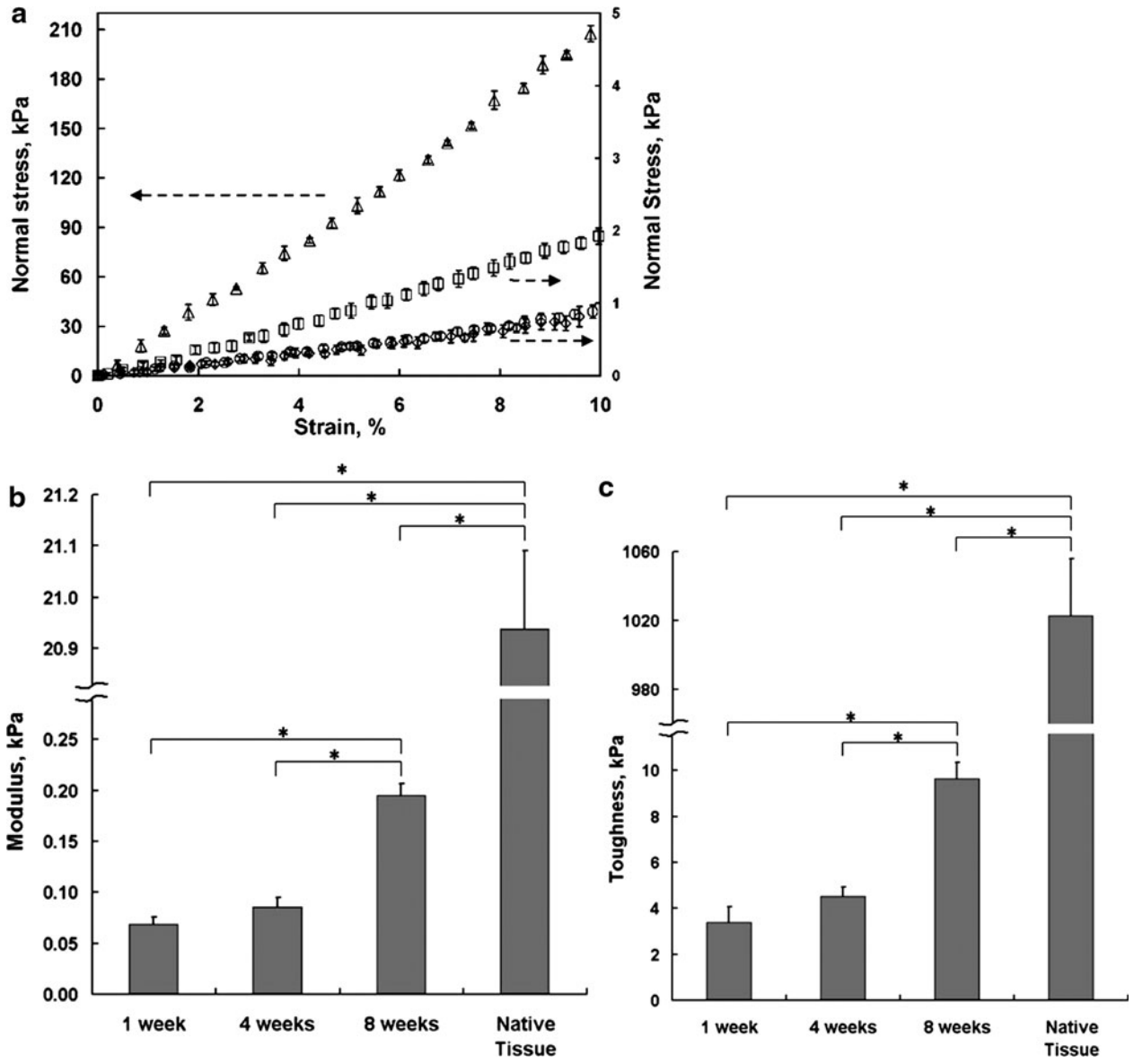

FIG. 10. Biomechanical properties of engineered tissue constructs and native osteochondral tissue under unconfined compression. Normal stress versus strain behavior under 10% compression (**a**), and corresponding modulus (**b**) and toughness (**c**) values. Symbol * indicates significance at $p < 0.05$ for $n = 3$. Error bars represent s.e.m. at 95% confidence level. Symbols in (**a**): ◊, tissue constructs at 1 week; ○, at 4 weeks; □, at 8 weeks; Δ, the native tissue.

The formation of calcified cartilage region adjacent to the substrate and a hyaline-like zone above was observed.

More recently, Ng *et al.*[48] formed bilayered scaffolds with depth-varying compressive material properties and seeded zonal populations of chondrocytes. They observed that such bilayered constructs led to depth-dependent cellular and compressive mechanical inhomogeneity, similar to that of the native tissue. A microparticle-based scaffold fabrication technique was also introduced recently to create scaffolds with spatial control over active ingredients using uniform poly(D,L-lactide-co-glycolide) microspheres with the aim of demonstrating the usefulness of such macroscopic gradients for interfacial tissue regeneration.[49]

In this study, biomimetic scaffolds made of unitary nonwoven meshes that were incorporated with bioactive agents were fabricated and employed to probe their suitability for the selective differentiation of stem cells for osteochondral applications. The highly porous scaffolds consisted of nonwoven meshes with pore sizes ranging between 5 and 50 μm. This pore size range is considered to be appropriate for cell infiltration during culture.[50] The ability to generate continuous concentration gradients of bioactive agents is an improvement over the earlier studies in functional grading of fibrous tissue engineering scaffolds, which typically utilized only one bioactive, which could be applied only in very simplistic modes. For example, varying concentrations of only β-tricalcium phosphate from the top to bottom volumes of a nanofibrous mesh were previously achieved.[17] Similarly, Li *et al.*[51] demonstrated the grading of calcium phosphate along the length of a nonwoven mat of electrospun

nanofibers, and Phillips *et al*.[3] generated gradients of retrovirus encoding the osteogenic transcription factor Runx2/Cbfa1 in collagen scaffolds containing poly(L-lysine). However, to our knowledge there are no reports of the incorporation of two or more bioactives into nanofibrous scaffolds in a continuously graded manner.

The ability of incorporating multiple bioactive agents within a nanostructured mat, that is demonstrated here, should provide a greater degree of freedom in mimicking both the physical as well as biological structures of osteochondral interface. The monotonic increase of β-GP and the monotonic decrease of insulin from one side of the scaffold to the other is but one of the many types of gradations of the bioactive agents that are possible with the twin-screw extrusion and electrospinning process. This particular type of gradation was selected to better isolate the individual effects of the two bioactive agents as well as the effect of their combination to mineralization and the differentiation of h-ADSCs.

The rapid dissolution rate of β-GP is consistent with the rapid achievement of the elevated concentrations of Ca and phosphates that are required for the initiation of mineralization.[52] Insulin, on the other hand, is an amphiphilic peptide; that is, it has a hydrophobic core consisting of carbon-rich amino acids at its center and relatively hydrophilic outer surfaces consisting of charged amino acids.[53] This amphiphilic nature of insulin gives rise to reduced dissolution and diffusion rates. In the scaffolds, insulin concentration increased linearly from 0% to $23.2\% \pm 2.6\%$ by weight from one side of scaffold to the other, whereas the β-GP concentration decreased from $48.3\% \pm 2.8\%$ to 0% by weight along the same direction. Based on the time-dependent weight loss of PCL-only, insulin/PCL, and β-GP/PCL meshes after immersing into the media, the $23.2\% \pm 2.6\%$ insulin concentration in the mesh was calculated to supply $\sim 25\,\mu g/mL$ of insulin to cell culture media during the first 2 days of culturing. This concentration of insulin is appropriate because it is within the concentration range at which effective chondrogenic differentiation could be achieved.[19,20,54] Concentrations of insulin $<40\,\mu g/mL$ were determined to promote chondrogenesis, whereas larger quantities ($>40\,\mu g/mL$) were found to downregulate the rate of chondrogenesis.[19] The sensitivity of chondrogenesis to insulin concentration was determined to be principally due to the effect of insulin to reduce the number of cell membrane receptors progressively by forming internalized hormone–receptor complexes at relatively high concentrations.[54] Relatively high concentrations of β-GP were targeted because elevated local phosphate ion concentrations are required to induce mineralization.[24,25]

H&E staining results shown in Figure 5 indicated that the cells penetrated into the core of the scaffold and that the trend of increasing number density of chondrocytic cells (Fig. 7) (cells with characteristic round shapes[55]) is in line with the monotonic increase of insulin concentration, affected by the differences in local insulin concentration. This observation is consistent with earlier findings,[19,56,57] which have demonstrated the effectiveness of insulin for the differentiation of stem cells. The qualitative nature of the distribution of the chondrocytic cell numbers is similar to what is observed to occur at the native cartilage–bone interface. McLauchlan and Gardner characterized human articular cartilage as a function of thickness and found that the density of chondrocytes declined from the superficial zone to the bone.[2]

Sulfated GAG was characterized and quantified throughout the thickness of tissue constructs using AB dye.[58] Since GAG is present in articular cartilage as a side chain of proteoglycans, which are important determinants of cartilage mechanical properties,[59] deposition of GAG (Fig. 8a) within our engineered tissue constructs indicates the development of a cartilage-like structure. However, there was no statistically significant dependence of GAG ($p > 0.05$) on the local insulin concentration (Fig. 8b). Collagen type II and type I are widely utilized to mark the chondrogenic[60–63] and osteogenic[64–66] phenotypes, respectively. Collagen is the most abundant macromolecule component (about 60% of the dry weight) in the articular cartilage. Particularly, the type II collagen represents 90% to 95% of the total collagen in cartilage ECM, whereas other types (I, IV, V, VI, IX, and XI) constitute only a minor proportion.[67] With regard to bone tissue, the major collagen type is found to be predominantly type I.[68,69] To probe the effects of the insulin gradient further, the tissue constructs of this study were stained with picrosirius red stain,[70] which binds to the collagen types I, II, and III (Fig. 8c). The semi-quantitative analysis of the picrosirius red stain results (Fig. 8d) revealed a statistically significant change in the stain intensity with scaffold thickness. The total collagen indeed increased with increasing distance toward the insulin-rich side. Thus, picrosirius red staining revealed significant increases in collagen synthesis with increasing insulin concentrations following the insulin gradient that was built into the scaffold (Fig. 8d), on the basis of chondrogenic differentiation as well as stimulative effect of insulin. Chondrogenically differentiated ADSCs were previously reported to produce more GAG and collagen than ADSCs controls,[71–73] suggesting that the graded collagen and GAG contents found in the tissue constructs of this study are attributable to the gradients of chondrogenically differentiated cells occurring as a result of the graded insulin concentration. This is actually consistent with the study of Musselmann *et al.*, who have shown that insulin alone stimulates the collagen synthesis *in vitro*.[74] Concomitant examination of the H&E staining results of Figure 5 and the total collagen distribution given in Figure 8c and d suggest that h-ADSCs penetrated across the entire cross section of the scaffold and that the distribution of the collagen deposition developed as a function of the insulin concentration distribution.

The differentiation of h-ADSCs was also confirmed by immunostaining of tissue constructs for MIA, that is, a cartilage-derived retinoic acid-sensitive protein that has been used as a marker for chondrocytic differentiation.[33] Under physiological condition, MIA is expressed only during the course of chondrogenesis through development and in mature chondrocytes and is not observed in other non-cartilaginous tissues.[30,31,75] Although MIA is pathologically expressed in malignant melanoma, minimal expression was detected in normal melanocytes.[76] In addition, it was found that MIA-deficient mice developed structural abnormalities in cartilage.[77] MIA is co-regulated with type II collagen in both expression *in vivo* and tissue distribution.[30–32] Similarly, differentiated chondrocytes in cell culture co-express MIA and collagen II.[33] In addition to examining MIA, we also detected increasing intensity of FGFR3 with increasing in-

sulin concentration (Fig. 6). FGFR3 is one of molecular markers during chondrogenesis and chondrocyte differentiation.[38] FGFR3-null mice are defective in articular cartilage with early arthritis.[78] Further, its expression correlates with collagen II by differentiated chondrocytes.[34] The observation of increasing FGFR3 intensity with increasing insulin concentration thus provided additional validation of the greater rate of differentiation of h-ADSCs into chondrogenic phenotype with increasing insulin concentration.

Differentiated chondrocytes are characteristically unstable by undergoing dedifferentiation and/or re-differentiation.[39–43] Phenotypic stability of chondrocytes was also evaluated by immunostaining the tissue constructs with ALK-1, a receptor involved in hypertrophic maturation of chondrocytes[79] and a marker of dedifferentiated chondrocytes.[34] Thus, we also stained ALK-1 to evaluate the phenotypic stability of the differentiated chondrocytes. Interestingly, ALK-1 was immunodetected in two morphologically distinctive cell populations in the 8-week tissue constructs corresponding to the gradient of insulin and β-GP. These results indicate that partial dedifferentiation occurred after chondrogenesis; however, a large portion of stable chondrogenic population remained in tissue constructs after 8 weeks in culture.

Regarding the effect of β-GP, the scaffold regions that were richer in the concentration of β-GP gave rise to greater mineral deposition at the same location as revealed by von Kossa staining. This finding is in agreement with the results of Allan *et al.*, who utilized β-GP for the mineralization of biphasic constructs comprised of cartilaginous tissue anchored to the top surface of a bone substrate.[23] The exact mechanism by which β-GP induces mineralization is unclear.[52] Generally, it is accepted that organic phosphate is hydrolyzed by alkaline phosphatase, an enzyme found on cell membrane of bone cells, to release free inorganic phosphate (iP), thus providing a chemical potential for mineral deposition. The iP is believed to induce mineralization either by direct mineral deposition due to elevated local iP concentration[24,80] or by metabolic process involving protein and RNA synthesis.[52,81–83]

In the characterization of biomechanical properties of cartilage tissue as well as engineered tissue constructs, in general, the aggregate modulus and the permeability are characterized as the parameters of well-studied cartilage biphasic model.[84] Here the unconfined compression technique, that is, similar to the characterization of tensile properties of the constructs in the radial direction along with the compressive properties in the thickness direction,[85] was used primarily on the basis of analogies between physiological contact loading and unconfined compression.[86] Elastic modulus (slope of stress versus strain curve in the linear range) and area under stress versus strain curve of tissue constructs were previously reported to be indicators of extent of mineralization and collagen formation, respectively.[87,88] The significantly higher modulus and area under stress versus strain curve values obtained after 8 weeks of cell culture as compared to those obtained after 1 and 4 weeks, therefore, suggest a considerable degree of tissue formation within 8 weeks.

In summary, the recently developed hybrid extrusion/electrospinning process was successfully implemented for generating tissue engineering scaffolds with controlled gradations of concentrations of insulin and β-GP. To our knowledge, this is the first time that multiple bioactive ingredients were incorporated in a distributed manner in nanofibrous-type biomimetic scaffolds. In this demonstration study, the concentration distributions were tailored so that the concentration of insulin increased monotonically from one side of scaffold to the other, whereas β-GP phosphate concentration decreased monotonically in the same direction. The use of both insulin and β-GP in conjunction with their systematically varied concentrations led to the differentiation of h-ADSCs in a location-dependent manner (higher chondrocytic cell counts and increasing total collagen deposition with increasing concentration of insulin) and different extents of mineralization as generated by the β-GP concentration distribution. The twin-screw extrusion electrospinning process, with its myriad capabilities for the tailoring of spatial physical and chemical properties in the tissue engineering scaffolds, should serve as another enabler for the mimicking of the gradations found in native tissues. We anticipate that the potential of the new fabrication method in generating realistic functionally graded scaffolds will be recognized by other investigators who would utilize such graded scaffolds *in vivo* to demonstrate the true benefits of functional grading.

Acknowledgments

We are grateful to Material Processing & Research Inc. of Hackensack, NJ, for making their MPR 7.5 mm twin-screw extrusion platform available to us. We thank David K. Moscatello from Coriell Institute for Medical Research (Camden, NJ) for providing the human adipose stromal cell line. We thank Dr. Halil Gevgilili of Highly Filled Materials Institute for his contributions to the development of the hybrid technology. We are also thankful to Markus F. Meyenhofer for his help in histological analyses, to Dr. Yelda Sertdemir Erisken for statistical evaluations, and to Prof. Xiaojun Yu of Stevens and Prof. Helen Lu of Columbia University for their help, feedback, and comments.

Disclosure Statement

No competing financial interests exist.

References

1. Moffat, K.L., Sun, W.H., Pena, P.E., Chahine, N.O., Doty, S.B., Ateshian, G.A., Hung, C.T., and Lu, H.H. Characterization of the structure-function relationship at the ligament-to-bone interface. Proc Natl Acad Sci USA **105,** 7947, 2008.
2. McLauchlan, G.J., and Gardner, D.L. Sacral and iliac articular cartilage thickness and cellularity: relationship to subchondral bone end-plate thickness and cancellous bone density. Rheumatology **41,** 375, 2002.
3. Phillips, J.E., Burns, K.L., Le Doux, J.M., Guldberg, R.E., and Garcia, A.J. Engineering graded tissue interfaces. Proc Natl Acad Sci USA **105,** 12170, 2008.
4. Bradley, D.A., Muthuvelu, P., Ellis, R.E., Green, E.M., Attenburrow, D., Barrett, R., Arkill, K., Colridge, D.B., and Winlove, C.P. Characterisation of mineralisation of bone and cartilage: X-ray diffraction and Ca and SrK alpha X-ray fluorescence microscopy. Nucl Instrum Meth B **263,** 1, 2007.
5. Jiang, J., Nicoll, S.B., and Lu, H.H. Co-culture of osteoblasts and chondrocytes modulates cellular differentiation *in vitro*. Biochem Biophys Res Commun **338,** 762, 2005.

6. Sarazin, P., Roy, X., and Favis, B.D. Controlled preparation and properties of porous poly(L-lactide) obtained from a cocontinuous blend of two biodegradable polymers. Biomaterials **25,** 5965, 2004.
7. Ozkan, S., Kalyon, D.M., Yu, X., McKelvey C., and Lowinger, M. Multifunctional polycaprolactone (PCL) scaffolds integrated for controlled release and tissue engineering: In vitro evaluation of released protein secondary structure stability, release profile and biocompatibility. Biomaterials **30**, 4336, 2009.
8. Luo, Y., Kobler, J.B., Zeitels, S.M., and Langer, R. Effects of growth factors on extracellular matrix production by vocal fold fibroblasts in 3-dimensional culture. Tissue Eng **12,** 3365, 2006.
9. Langer, R., and Vacanti, J.P. Tissue Engineering. Science **260,** 920, 1993.
10. Uebersax, L., Merkle, H.P., and Meinel, L. Insulin-like growth factor I releasing silk fibroin scaffolds induce chondrogenic differentiation of human mesenchymal stem cells. J Control Release **127,** 12, 2008.
11. Li, C., Vepari, C., Jin, H.J., Kim, H.J., and Kaplan, D.L. Electrospun silk-BMP-2 scaffolds for bone tissue engineering. Biomaterials **27,** 3115, 2006.
12. Levenberg, S., Huang, N.F., Lavik, E., Rogers, A.B., Itskovitz-Eldor, J., and Langer, R. Differentiation of human embryonic stem cells on three-dimensional polymer scaffolds. Proc Natl Acad Sci USA **100,** 12741, 2003.
13. Wang, X., Wenk, E., Zhang, X., Meinel, L., Vunjak-Novakovic, G., and Kaplan, D.L. Growth factor gradients via microsphere delivery in biopolymer scaffolds for osteochondral tissue engineering. J Control Release **134,** 81, 2009.
14. Benoit, D.S., Schwartz, M.P., Durney, A.R., and Anseth, K.S. Small functional groups for controlled differentiation of hydrogel-encapsulated human mesenchymal stem cells. Nat Mater **7,** 816, 2008.
15. Archer, R., and Williams, D.J. Why tissue engineering needs process engineering. Nat Biotechnol **23,** 1353, 2005.
16. Erisken, C., Kalyon, D.M., and Wang, H.J. A hybrid twin screw extrusion/electrospinning method to process nanoparticle-incorporated electrospun nanofibres. Nanotechnology **19,** 165302, 2008.
17. Erisken, C., Kalyon, D.M., and Wang, H. Functionally graded electrospun polycaprolactone and beta-tricalcium phosphate nanocomposites for tissue engineering applications. Biomaterials **29,** 4065, 2008.
18. Zuk, P.A., Zhu, M., Mizuno, H., Huang, J., Futrell, J.W., Katz, A.J., Benhaim, P., Lorenz, H.P., and Hedrick, M.H. Multilineage cells from human adipose tissue: implications for cell-based therapies. Tissue Eng **7,** 211, 2001.
19. Hadhazy, C., and Dedukh, N.V. [Effect of insulin on cartilage differentiation *in vitro*]. Biull Eksp Biol Med **105,** 219, 1988.
20. Julian, D., and Abbott, U.K. An avian model for comparative studies of insulin teratogenicity. Anat Histol Embryol **27,** 313, 1998.
21. Marolt, D., Augst, A., Freed, L.E., Vepari, C., Fajardo, R., Patel, N., Gray, M., Farley, M., Kaplan, D., and Vunjak-Novakovic, G. Bone and cartilage tissue constructs grown using human bone marrow stromal cells, silk scaffolds and rotating bioreactors. Biomaterials **27,** 6138, 2006.
22. Maor, G., Silbermann, M., von der, M.K., Heingard, D., and Laron, Z. Insulin enhances the growth of cartilage in organ and tissue cultures of mouse neonatal mandibular condyle. Calcif Tissue Int **52,** 291, 1993.
23. Allan, K.S., Pilliar, R.M., Wang, J., Grynpas, M.D., and Kandel, R.A. Formation of biphasic constructs containing cartilage with a calcified zone interface. Tissue Eng **13,** 167, 2007.
24. Chung, C.H., Golub, E.E., Forbes, E., Tokuoka, T., and Shapiro, I.M. Mechanism of action of beta-glycerophosphate on bone cell mineralization. Calcif Tissue Int **51,** 305, 1992.
25. Tenenbaum, H.C. Role of organic phosphate in mineralization of bone *in vitro*. J Dent Res **60 Spec No C,** 1586, 1981.
26. Wall, M.E., Rachlin, A., Otey, C.A., and Loboa, E.G. Human adipose-derived adult stem cells upregulate palladin during osteogenesis and in response to cyclic tensile strain. Am J Physiol Cell Physiol **293,** C1532, 2007.
27. Wu, Y.N., Yang, Z., Hui, J.H., Ouyang, H.W., and Lee, E.H. Cartilaginous ECM component-modification of the microbead culture system for chondrogenic differentiation of mesenchymal stem cells. Biomaterials **28,** 4056, 2007.
28. Erisken, C., Kalyon, D.M., and Wang, H. Viscoelastic and biomechanical properties of osteochondral tissue constructs generated from graded polycaprolactone and beta-tricalcium phosphate composites. J Biomech Eng **132,** 091013, 2010.
29. Lemke, M.J., Churchill, P.F., and Wetzel, R.G. Effect of substrate and cell surface hydrophobicity on phosphate utilization in bacteria. Appl Environ Microbiol **61,** 913, 1995.
30. Kondo, S., Xie, W.-F., Cha, S.H., and Sandell, L.J. Discovery and characteristic features of cartilage-derived retinoic acid-sensitive protein (CD-RAP). Eur Cells Mater **8,** 57, 1998.
31. Sakano, S., Zhu, Y., and Sandell, L.J. Cartilage-derived retinoic acid-sensitive protein and type II collagen expression during fracture healing are potential targets for Sox9 regulation. J Bone Miner Res **14,** 1891, 1999.
32. Dietz, U.H., and Sandell, L.J. Cloning of a retinoic acid-sensitive mRNA expressed in cartilage and during chondrogenesis. J Biol Chem **271,** 3311, 1996.
33. Bosserhoff, A.K., and Buettner, R. Establishing the protein MIA (melanoma inhibitory activity) as a marker for chondrocyte differentiation. Biomaterials **24,** 3229, 2003.
34. Dell'Accio, F., De Bari, C., and Luyten, F.P. Molecular markers predictive of the capacity of expanded human articular chondrocytes to form stable cartilage *in vivo*. Arthritis Rheum **44,** 1608, 2001.
35. Deng, C., Wynshaw-Boris, A., Zhou, F., Kuo, A., and Leder, P. Fibroblast growth factor receptor 3 is a negative regulator of bone growth. Cell **84,** 911, 1996.
36. Colvin, J.S., Bohne, B.A., Harding, G.W., McEwen, D.G., and Ornitz, D.M. Skeletal overgrowth and deafness in mice lacking fibroblast growth factor receptor 3. Nat Genet **12,** 390, 1996.
37. Su, N., Yang, J., Xie, Y., Du, X., Lu, X., Yin, Z., Yin, L., Qi, H., Zhao, L., Feng, J., and Chen, L. Gain-of-function mutation of FGFR3 results in impaired fracture healing due to inhibition of chondrocyte differentiation. Biochem Biophys Res Commun **376,** 454, 2008.
38. Zuscik, M.J., Hilton, M.J., Zhang, X., Chen, D., and O'Keefe, R.J. Regulation of chondrogenesis and chondrocyte differentiation by stress. J Clin Invest **118,** 429, 2008.
39. Ghosh, P., and Smith, M. Osteoarthritis, genetic and molecular mechanisms. Biogerontology **3,** 85, 2002.
40. Lefebvre, V., Peeters-Joris, C., and Vaes, G. Modulation by interleukin 1 and tumor necrosis factor alpha of production of collagenase, tissue inhibitor of metalloproteinases and collagen types in differentiated and dedifferentiated articular chondrocytes. Biochim Biophys Acta **1052,** 366, 1990.
41. Benya, P.D., Padilla, S.R., and Nimni, M.E. The progeny of rabbit articular chondrocytes synthesize collagen types I and

III and type I trimer, but not type II. Verifications by cyanogen bromide peptide analysis. Biochemistry **16,** 865, 1977.
42. Yoon, Y.M., Kim, S.J., Oh, C.D., Ju, J.W., Song, W.K., Yoo, Y.J., Huh, T.L., and Chun, J.S. Maintenance of differentiated phenotype of articular chondrocytes by protein kinase C and extracellular signal-regulated protein kinase. J Biol Chem **277,** 8412, 2002.
43. Bonaventure, J., Kadhom, N., Cohen-Solal, L., Ng, K.H., Bourguignon, J., Lasselin, C., and Freisinger, P. Reexpression of cartilage-specific genes by dedifferentiated human articular chondrocytes cultured in alginate beads. Exp Cell Res **212,** 97, 1994.
44. Woodfield, T.B., van Blitterswijk, C.A., De, W.J., Sims, T.J., Hollander, A.P., and Riesle, J. Polymer scaffolds fabricated with pore-size gradients as a model for studying the zonal organization within tissue-engineered cartilage constructs. Tissue Eng **11,** 1297, 2005.
45. Leong, K.F., Chua, C.K., Sudarmadji, N., and Yeong, W.Y. Engineering functionally graded tissue engineering scaffolds. J Mech Behav Biomed Mater **1,** 140, 2008.
46. Schaefer, D., Martin, I., Shastri, P., Padera, R.F., Langer, R., Freed, L.E., and Vunjak-Novakovic, G. *In vitro* generation of osteochondral composites. Biomaterials **21,** 2599, 2000.
47. Sherwood, J.K., Riley, S.L., Palazzolo, R., Brown, S.C., Monkhouse, D.C., Coates, M., Griffith, L.G., Landeen, L.K., and Ratcliffe, A. A three-dimensional osteochondral composite scaffold for articular cartilage repair. Biomaterials **23,** 4739, 2002.
48. Ng, K.W., Ateshian, G.A., and Hung, C.T. Zonal Chondrocytes seeded in a layered agarose hydrogel create engineered cartilage with depth-dependent cellular and mechanical inhomogeneity. Tissue Eng Part A **15,** 2315, 2009.
49. Singh, M., Morris, C.P., Ellis, R.J., Detamore, M.S., and Berkland, C. Microsphere-based seamless scaffolds containing macroscopic gradients of encapsulated factors for tissue engineering. Tissue Eng Part C Methods **14,** 299, 2008.
50. Zeltinger, J., Sherwood, J.K., Graham, D.A., Mueller, R., and Griffith, L.G. Effect of pore size and void fraction on cellular adhesion, proliferation, and matrix deposition. Tissue Eng **7,** 557, 2001.
51. Li, X.R., Xie, J.W., Lipner, J., Yuan, X.Y., Thomopoulos, S., and Xia, Y.N. Nanofiber scaffolds with gradations in mineral content for mimicking the tendon-to-bone insertion site. Nano Lett **9,** 2763, 2009.
52. Chang, Y.L., Stanford, C.M., and Keller, J.C. Calcium and phosphate supplementation promotes bone cell mineralization: implications for hydroxyapatite (HA)-enhanced bone formation. J Biomed Mater Res **52,** 270, 2000.
53. Yu, H., and Grainger, D.W. Modified release of hydrophilic, hydrophobic and peptide agents from ionized amphiphilic gel networks. J Control Release **34,** 117, 1995.
54. Serravezza, J.C., Endo, F., Dehaan, R.L., and Elsas, L.J. Insulin-induced receptor loss reduces responsiveness of chick heart-cells to insulin. Endocrinology **113,** 497, 1983.
55. Bhattarai, N., Edmondson, D., Veiseh, O., Matsen, F.A., and Zhang, M.Q. Electrospun chitosan-based nanofibers and their cellular compatibility. Biomaterials **26,** 6176, 2005.
56. Kemp, S.F., Mutchnick, M., and Hintz, R.L. Hormonal-control of protein-synthesis in chick chondrocytes—a comparison of effects of insulin, somatomedin-c and triiodothyronine. Acta Endocrinol **107,** 179, 1984.
57. Muramatsu, T., Kita, K., Nakagawa, S., and Okumura, J. Effects of insulin, growth-hormone, IGF-I and IGF-II on phenylalanine extraction in the chicken-embryo cultured *in vitro*. Comp Biochem Physiol A Physiol **104,** 507, 1993.
58. Scott, J.E., and Dorling, J. Differential staining of acid glycosaminoglycans (mucopolysaccharides) by alcian blue in salt solutions. Histochemie **5,** 221, 1965.
59. Zhu, W., Mow, V.C., Koob, T.J., and Eyre, D.R. Viscoelastic shear properties of articular cartilage and the effects of glycosidase treatments. J Orthop Res **11,** 771, 1993.
60. Steinert, A., Weber, M., Dimmler, A., Julius, C., Schutze, N., Noth, U., Cramer, H., Eulert, J., Zimmermann, U., and Hendrich, C. Chondrogenic differentiation of mesenchymal progenitor cells encapsulated in ultrahigh-viscosity alginate. J Orthop Res **21,** 1090, 2003.
61. Neumann, K., Dehne, T., Endres, M., Erggelet, C., Kaps, C., Ringe, J., and Sittinger, M. Chondrogenic differentiation capacity of human mesenchymal progenitor cells derived from subchondral cortico-spongious bone. J Orthop Res **26,** 1449, 2008.
62. Junker, J.P.E., Sommar, P., Skog, M., Johnson, H., and Kratz, G. Adipogenic, chondrogenic and osteogenic differentiation of clonally derived human dermal fibroblasts. Cells Tissues Organs **191,** 105, 2010.
63. Williams, R., Khan, I.M., Richardson, K., Nelson, L., McCarthy, H.E., Analbelsi, T., Singhrao, S.K., Dowthwaite, G.P., Jones, R.E., Baird, D.M., Lewis, H., Roberts, S., Shaw, H.M., Dudhia, J., Fairclough, J., Briggs, T., and Archer, C.W. Identification and clonal characterisation of a progenitor cell sub-population in normal human articular cartilage. PLoS ONE **5,** e13246, 2010.
64. Garreta, E., Genove, E., Borros, S., and Semino, C.E. Osteogenic differentiation of mouse embryonic stem cells and mouse embryonic fibroblasts in a three-dimensional self-assembling peptide scaffold. Tissue Eng **12,** 2215, 2006.
65. Knabe, C., Kraska, B., Koch, C., Gross, U., Zreiqat, H., and Stiller, M. A method for immunohistochemical detection of osteogenic markers in undecalcified bone sections. Biotech Histochem **81,** 31, 2006.
66. Schutze, N., Noth, U., Schneidereit, J., Hendrich, C., and Jakob, F. Differential expression of CCN-family members in primary human bone marrow-derived mesenchymal stem cells during osteogenic, chondrogenic and adipogenic differentiation. Cell Commun Signal **3,** 5, 2005.
67. Sophia Fox, A.J., Bedi, A., and Rodeo, S.A. The basic science of articular cartilage: structure, composition, and function. Sports Health: A Multidisciplinary Approach **1,** 461, 2009.
68. Barsh, G.S., David, K.E., and Byers, P.H. Type I osteogenesis imperfecta: a nonfunctional allele for pro alpha 1 (I) chains of type I procollagen. Proc Natl Acad Sci USA **79,** 3838, 1982.
69. Kirsch, E., Krieg, T., Nerlich, A., Remberger, K., Meinecke, P., Kunze, D., and Muller, P.K. Compositional analysis of collagen from patients with diverse forms of osteogenesis imperfecta. Calcif Tissue Int **41,** 11, 1987.
70. Junqueira, L.C., Bignolas, G., and Brentani, R.R. Picrosirius staining plus polarization microscopy, a specific method for collagen detection in tissue sections. Histochem J **11,** 447, 1979.
71. Zuk, P.A., Zhu, M., Ashjian, P., De Ugarte, D.A., Huang, J.I., Mizuno, H., Alfonso, Z.C., Fraser, J.K., Benhaim, P., and Hedrick, M.H. Human adipose tissue is a source of multipotent stem cells. Mol Biol Cell **13,** 4279, 2002.
72. Awad, H.A., Wickham, M.Q., Leddy, H.A., Gimble, J.M., and Guilak, F. Chondrogenic differentiation of

adipose-derived adult stem cells in agarose, alginate, and gelatin scaffolds. Biomaterials **25,** 3211, 2004.
73. Tapp, H., Deepe, R., Ingram, J.A., Kuremsky, M., Hanley, E.N., Jr., and Gruber, H.E. Adipose-derived mesenchymal stem cells from the sand rat: transforming growth factor beta and 3D co-culture with human disc cells stimulate proteoglycan and collagen type I rich extracellular matrix. Arthritis Res Ther **10,** R89, 2008.
74. Musselmann, K., Kane, B., Alexandrou, B., and Hassell, J.R. Stimulation of collagen synthesis by insulin and proteoglycan accumulation by ascorbate in bovine keratocytes *in vitro*. Invest Ophthalmol Vis Sci **47,** 5260, 2006.
75. Bosserhoff, A.K., Kondo, S., Moser, M., Dietz, U.H., Copeland, N.G., Gilbert, D.J., Jenkins, N.A., Buettner, R., and Sandell, L.J. Mouse CD-RAP/MIA gene: structure, chromosomal localization, and expression in cartilage and chondrosarcoma. Dev Dyn **208,** 516, 1997.
76. Guba, M., Bosserhoff, A.K., Steinbauer, M., Abels, C., Anthuber, M., Buettner, R., and Jauch, K.W. Overexpression of melanoma inhibitory activity (MIA) enhances extravasation and metastasis of A-mel 3 melanoma cells *in vivo*. Br J Cancer **83,** 1216, 2000.
77. Moser, M., Bosserhoff, A.K., Hunziker, E.B., Sandell, L., Fassler, R., and Buettner, R. Ultrastructural cartilage abnormalities in MIA/CD-RAP-deficient mice. Mol Cell Biol **22,** 1438, 2002.
78. Valverde-Franco, G., Binette, J.S., Li, W., Wang, H., Chai, S., Laflamme, F., Tran-Khanh, N., Quenneville, E., Meijers, T., Poole, A.R., Mort, J.S., Buschmann, M.D., and Henderson, J.E. Defects in articular cartilage metabolism and early arthritis in fibroblast growth factor receptor 3 deficient mice. Hum Mol Genet **15,** 1783, 2006.
79. Valcourt, U., Gouttenoire, J., Moustakas, A., Herbage, D., and Mallein-Gerin, F. Functions of transforming growth factor-beta family type I receptors and smad proteins in the hypertrophic maturation and osteoblastic differentiation of chondrocytes. J Biol Chem **277,** 33545, 2002.
80. Tenenbaum, H.C. Levamisole and inorganic pyrophosphate inhibit beta-glycerophosphate induced mineralization of bone formed *in vitro*. Bone Miner **3,** 13, 1987.
81. Gough, J.E., Jones, J.R., and Hench, L.L. Nodule formation and mineralisation of human primary osteoblasts cultured on a porous bioactive glass scaffold. Biomaterials **25,** 2039, 2004.
82. Fujita, T., Meguro, T., Izumo, N., Yasutomi, C., Fukuyama, R., Nakamuta, H., and Koida, M. Phosphate stimulates differentiation and mineralization of the chondroprogenitor clone ATDC5. Jpn J Pharmacol **85,** 278, 2001.
83. Kandel, R.A., Boyle, J., Gibson, G., Cruz, T., and Speagle, M. *In vitro* formation of mineralized cartilagenous tissue by articular chondrocytes. In Vitro Cell Dev Biol Anim **33,** 174, 1997.
84. Wang, C.C., Hung, C.T., and Mow, V.C. An analysis of the effects of depth-dependent aggregate modulus on articular cartilage stress-relaxation behavior in compression. J Biomech **34,** 75, 2001.
85. Armstrong, C.G., Lai, W.M., and Mow, V.C. An analysis of the unconfined compression of articular cartilage. J Biomech Eng **106,** 165, 1984.
86. Park, S., Hung, C.T., and Ateshian, G.A. Mechanical response of bovine articular cartilage under dynamic unconfined compression loading at physiological stress levels. Osteoarthritis Cartilage **12,** 65, 2004.
87. Garnero, P., Borel, O., Gineyts, E., Duboeuf, F., Solberg, H., Bouxsein, M.L., Christiansen, C., and Delmas, P.D. Extracellular post-translational modifications of collagen are major determinants of biomechanical properties of fetal bovine cortical bone. Bone **38,** 300, 2006.
88. Burr, D.B. The contribution of the organic matrix to bone's material properties. Bone **31,** 8, 2002.

Address correspondence to:
Dilhan M. Kalyon, Ph.D.
Department of Chemical Engineering and Material Science and Department of Chemistry, Chemical Biology and Biomedical Engineering
Stevens Institute of Technology
McLean Chemical and Life Sciences Building
1 Castle Point on Hudson
Hoboken, NJ 07030

E-mail: dkalyon@stevens.edu

Received: October 21, 2009
Accepted: December 23, 2010
Online Publication Date: January 31, 2011